Proceedings of Meetings on Acoustics

Volume 19, 2013 http://acousticalsociety.org/

ICA 2013 Montreal
Montreal, Canada
2 - 7 June 2013

Structural Acoustics and Vibration
Session 5aSA: Applications in Structural Acoustics and Vibration IV

5aSA7. Multi-component power transmission from structure-borne sound sources into lightweight structures

Sebastian Mathiowetz* and Hannes A. Bonhoff

***Corresponding author's address: Institute of Fluid Mechanics and Engineering Acoustics, Technische Universität Berlin, Einsteinufer 25, Berlin, 10587, Berlin, Germany, s.mathiowetz@tu-berlin.de**

The power transmission between structure-borne sound sources and adjacent structures is generally of complex nature. For an accurate description the interaction between multiple contact points and several directional components must be taken into account. While calculation methods to predict the transmitted power are generally available, the main problem is the acquisition of extensive source and receiver data. This is especially true with regard to lightweight structures where source and receiver mobilities exhibit matched conditions and when rotational components of motion are involved. Therefore, the description needs to be simplified while at the same time a sufficient accuracy has to be retained. This work investigates the power transmission of a fan unit source that is mounted to a rib-stiffened aluminium plate at several contact points. Full data sets of source and receiver have been measured using a finite difference technique, including translational motion perpendicular to the structure as well as moment excitation around the in-plane axes of the plate. Both a rigid connection as well as a connection using resilient mounts are considered. Contributions of different components of motion are discussed and possible simplifications are deduced.

Published by the Acoustical Society of America through the American Institute of Physics

 [DOI: 10.1121/1.4799705]
Received 22 Jan 2013; published 2 Jun 2013

INTRODUCTION

Lightweight structures are commonly used in the industry as they provide an optimized balance between weight and stiffness. In the shipbuilding sector, rib-stiffened plates in various configurations occur as a basic construction. However, the benefit of reduced weight is detrimental when a structure-borne sound source is installed, injecting sound power into the structure.

A source is generally connected at several contact points to a receiver, and different components of motion can be involved. Rotatory components may be of influence particularly at structural discontinuities and their relative importance increases with frequency [1], [2]. In order to obtain the power injected into the receiver, extensive input data in form of source and receiver mobility matrices as well as the source activity are required. For noise prediction on board ships it is therefore valuable to know if and how the description can be simplified properly, and second, which errors have to be expected when simplifications are introduced.

In recently published work [3] concerning the structure-borne sound transmission from sources into a lightweight point-connected timber joist floor construction it was shown that motion perpendicular to the structure dominates. Furthermore, an expression for the transmitted power in terms of single equivalent values derived as spatial averages of source and receiver properties was developed. Hereby the description of the transmission process is radically simplified. Especially for manufacturers or consulting engineers concerned with noise issues, a single-value description is desirable.

This paper addresses the structure-borne sound transmission from a fan unit source connected at four contact points to a continuously welded rib-stiffened aluminum plate. The translational motion component perpendicular to the receiver plate accounted for by the force F_z and velocity v_z and rotatory motion components around the in-plane axes of the plate accounted for by moments M_x, M_y and rotatory velocities w_x, w_y are considered. The discrepancy between an exact calculation of power involving translational and rotatory components and a calculation reduced to the translational component is investigated. A rigid connection as well as a connection with resilient mounts are considered. Secondly, the approach of single equivalent approximation [3] and a neglect of source mobility are tested for the resiliently mounted case. Data sets of source and receiver mobilities as well as the free velocities were measured while the mobilities of the isolators were calculated approximately from theory.

THEORETICAL BACKGROUND

Power Transmission

In order to account for the interaction of contact points and/or motion components with regard to structure-borne sound power transmission, a matrix description can be used. The transmitted power then can be calculated from source and receiver mobility matrices $\mathbf{Y}_S$ and $\mathbf{Y}_R$ and from the activity of the source, represented by the free velocity vector $\mathbf{v}_{SF}$. Throughout this paper, lower case bold letters indicate vector notation while upper case bold letters indicate matrices. In the case of a rigid connection between source and receiver, the transmitted power is obtained by [4]

$$W = \frac{1}{2} Re\{\mathbf{v}_{SF}^T (\mathbf{Y}_S + \mathbf{Y}_R)^{-T} \mathbf{Y}_R^T (\mathbf{Y}_S^* + \mathbf{Y}_R^*)^{-1} \mathbf{v}_{SF}^*\}. \quad (1)$$

Here, superscripts -1 indicate a matrix inversion, T the transpose and $*$ the complex conjugate. When the source is installed on resilient mounts at each contact point, the dynamic properties of

the isolators have to be included in the formulation. The mobility matrix $\mathbf{Y}_{I,n}$ of each n^{th} isolator can be written in complete (cf. [5]) or compact form, respectively, as

$$\mathbf{Y}_{I,n} = \begin{bmatrix} Y^{v_zF_z}_{I,SS,n} & 0 & 0 & Y^{v_zF_z}_{I,SR,n} & 0 & 0 \\ 0 & Y^{w_xM_x}_{I,SS,n} & 0 & 0 & Y^{w_xM_x}_{I,SR,n} & 0 \\ 0 & 0 & Y^{w_yM_y}_{I,SS,n} & 0 & 0 & Y^{w_yM_y}_{I,SR,n} \\ Y^{v_zF_z}_{I,RS,n} & 0 & 0 & Y^{v_zF_z}_{I,RR,n} & 0 & 0 \\ 0 & Y^{w_xM_x}_{I,RS,n} & 0 & 0 & Y^{w_xM_x}_{I,RR,n} & 0 \\ 0 & 0 & Y^{w_yM_y}_{I,RS,n} & 0 & 0 & Y^{w_yM_y}_{I,RR,n} \end{bmatrix} = \begin{bmatrix} \mathbf{Y}_{I,SS,n} & \mathbf{Y}_{I,SR,n} \\ \mathbf{Y}_{I,RS,n} & \mathbf{Y}_{I,RR,n} \end{bmatrix}. \tag{2}$$

In Eq. 2, indices SS and RR indicate excitation and response at the source or receiver end of the isolator, respectively. Indices SR indicate an excitation at the receiver end and response at the source end, while RS indicate an excitation at the source end and response at the receiver end. The notation of field variables for an isolator can be taken from Fig. 1.

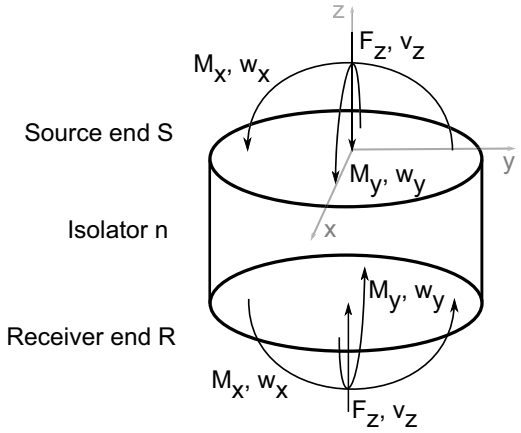

FIGURE 1: Notation of field variables for isolator scheme

In order to integrate the isolator mobilities in the power formulation from Eq. (1) they must be reassembled to fit to the structure of source and receiver mobility matrices. Hence, four mobility matrices $\mathbf{Y}_{I,SS}, \mathbf{Y}_{I,RR}$, $\mathbf{Y}_{I,SR}$ and $\mathbf{Y}_{I,RS}$ that contain the respective submatrices from $\mathbf{Y}_{I,n}$ with $n = 1,2,3,4$ on the diagonal are assembled. As the isolators are placed at each contact point, transfer mobilities of the isolator matrices that account for a coupling between the contact points are equal to zero. The transmitted power for a resiliently mounted source then can be written as

$$W = \frac{1}{2} Re\{\mathbf{v}_{SF}^T \mathbf{Y}_{I,RS}^T \mathbf{A}^{-T} \mathbf{Y}_R^T \mathbf{A}^{-*} \mathbf{Y}_{I,RS}^* \mathbf{v}_{SF}^*\} \tag{3}$$

$$\text{with } \mathbf{A} = \mathbf{Y}_{I,RS}(\mathbf{Y}_{I,SS} + \mathbf{Y}_S)\mathbf{Y}_{I,RS}^{-1}(\mathbf{Y}_{I,RR} + \mathbf{Y}_R) - \mathbf{Y}_{I,RS}\mathbf{Y}_{I,SR}.$$

Single equivalent approximation

The concept of single equivalent approximation [3] provides a single value description of source and receiver mobilities and of the source activity on condition that the translational motion component perpendicular to the structure dominates. Based on the concept of effective mobilities [6], [7], single equivalent values can be calculated from source and receiver mobility matrices and from the source activity vector, respectively. The effective mobility at a contact point n and in one component of motion is calculated by superposition of the driving point mobility at n and the contributions of velocities at n caused by forces which act at points $m \neq n$:

$$Y_n^{\Sigma} = Y_{nn} + \sum_{m=1, m\neq n}^{N} Y_{nm} \frac{F_m}{F_n}. \tag{4}$$

As the contact forces in Eq. (4) are not known in general, assumptions about force distributions have to be made. It was shown that a unit force ratio can be assumed, even if the magnitude of force ratios varies in a range of ±10 dB about unity [8]. Additionally, an estimate of the phase distribution is required. A zero phase distribution is proposed at low frequencies where the source is acting in bouncing mode as a compact source. At higher frequencies where source or receiver structures show a resonant behavior, a random phase distribution is applicable [6]. Assuming unit magnitude and zero phase distribution, Eq. (4) becomes

$$Y_n^{\Sigma} = Y_{nn} + \sum_{m=1, m\neq n}^{N} Y_{nm}. \tag{5}$$

For unit magnitude and random phase distribution, only the magnitude of the effective mobility can be retained

$$|Y_n^{\Sigma}| = \sqrt{|Y_{nn}|^2 + \sum_{m=1, m\neq n}^{N} |Y_{nm}|^2}. \tag{6}$$

The single equivalent mobilities are derived by averaging the effective mobilities from either Eq. (5) or Eq. (6) over the N contact points:

$$Y_{eq}^{\Sigma} = \frac{1}{N} \sum_{n=1}^{N} Y_n^{\Sigma}. \tag{7}$$

The single equivalent source activity is derived as the sum of the squared free velocity magnitudes at the contact points $\sum_{n=1}^{N} |v_{SF,n}|^2$.

Including the dynamic properties of the isolators in the single equivalent approximation of the transmitted power is straightforward: As the isolators are placed at each contact point, there is no transfer coupling to be taken into account. The effective mobilities of the isolator point or transfer mobility matrices, $\mathbf{Y}_{I,RS}, \mathbf{Y}_{I,RR}, \mathbf{Y}_{I,SR}$ and $\mathbf{Y}_{I,RS}$, therefore are equivalent to the point and transfer mobilities of the isolators themselves and no assumptions about force ratios have to be made. Consequently, the single equivalent values of the isolator point- or transfer mobility matrices are derived as the spatial average of N isolator point or transfer mobilities according to Eq. (7) and denoted as $\overline{Y}_{I,SS}, \overline{Y}_{I,RR}, \overline{Y}_{I,SR}$ and $\overline{Y}_{I,RS}$. The transmitted power for the resiliently mounted source using single equivalent values can be written as

$$W_{eq} = \frac{1}{2} \sum_{n=1}^{N} |v_{SF,n}|^2 \frac{Re(Y_{R,eq}^{\Sigma}) |\overline{Y}_{I,RS}|^2}{(|Y_{R,eq}^{\Sigma} + \overline{Y}_{I,RR})(Y_{S,eq}^{\Sigma} + \overline{Y}_{I,SS}) + \overline{Y}_{I,RS}\overline{Y}_{I,SR}|^2}. \tag{8}$$

Test Setup

The installation consists of a fan unit source connected at four contact points to a continuously welded rib-stiffened aluminum plate. For the measurement of source mobility and free velocity, the fan unit was freely suspended, see Fig. 2 a. The footing structure of the fan unit is built from flange-like metal sheets on which the contact points are located. In order to broaden the validity of the results, a second fictitious contact condition was considered by attaching aluminum feet to the metal sheets by screws, see Fig. 2 b.

FIGURE 2: (a) Fan unit source, (b) Aluminum feet; left: with accelerometers mounted; right: dissembled foot shown from the bottom, (c) Stiffened plate in sand bed with 3 interface positions

The receiver consists of a homogeneous aluminum plate ($l \times w \times h = 3000\,\text{mm} \times 1500\,\text{mm} \times 8\,\text{mm}$) with four continuously welded aluminum joists ($l \times w \times h = 3000\,\text{mm} \times 8\,\text{mm} \times 100\,\text{mm}$) attached from below with a spacing of 450 mm from joist to joist, see Fig 2 c. The dotted lines indicate the locations of the joists. The receiver geometry was chosen in order to represent a typical base structure of rib-stiffened plates used in ship construction. In a real-life situation, the plate dimensions would be considerably larger. In order to approximate the real situation, global resonances of the plate were damped by embedding the plate edges in sand. Three interface positions were measured. At interface 1, two contact points are located centrally in a bay between two joists and two contact points are located centrally in the adjacent bay (see white markers in Fig. 2 c). At interface 2, all points are moved towards the stiffening joists (see gray markers in Fig. 2 c). In the case of interface 3, all contact points are located on a joist (see black markers in Fig. 2 c). In order to derive the translational and rotatory components of mobility matrices and free velocities, a finite difference technique [9] was applied. The approach provides a procedure where only translational point and transfer mobilities perpendicular to the structure have to be measured, from which translational and rotatory components can be derived by calculation. For the case that the source is connected to the plate by resilient mounts, elastomeric isolators are assumed. The single mobilities of the isolators in Eq. (2) are calculated approximately by using long-rod and thin-beam theory for the vertical and rotatory motion components, respectively. Solutions for all motion components can be found in [10], for instance. It was reported [5] that reliable results for the transmitted power can be obtained with this approach. With properly chosen material parameters for the isolators, the fundamental vertical rigid-body resonance of the source-isolator system occurs at about $f_{res} = 11\,\text{Hz}$.

RESULTS

Importance of Motion Components

In this section, the discrepancy between an exact calculation of power involving translational and rotatory components and a calculation from the translational component solely is investigated. In case of a rigid connection, the transmitted power is given by Eq. (1). In the resiliently mounted case, the transmitted power is given by Eq. (3).

In Fig. 3 (a) - (c) the transmitted power is shown for the three interface positions depicted in Fig. 2 (c) when the contact points are located on the metal sheets of the fan unit frame structure. Gray and black lines show the transmitted power for the rigidly and resiliently mounted case, respectively. Solid lines indicate a calculation including rotatory and translational components while dashed lines indicate a calculation from the translational component solely. Results are seen to be similar for any of the three interface positions. In the rigidly mounted case, rotatory

components gain importance from about $f = 800$ Hz onwards. Here, the exact transmitted power exceeds the power transmitted by the translational component by about 15 dB on average. In the frequency range below, the influence of rotatory components is significantly smaller and the power transmitted by the translational component approaches the exact transmitted power within a range of ±5 dB. At certain frequencies, the power transmitted by the vertical component exceeds the exact transmitted power. An explanation for that might be the occurence of measurement uncertainties and errors that stem from matrix inversions, likely to occur in the lower frequency range.

When isolators are introduced, the influence of rotatory components becomes negligible. Throughout the frequency range, the power calculated from the translational component underestimates the exact power involving translational and rotatory components by about 1 dB.

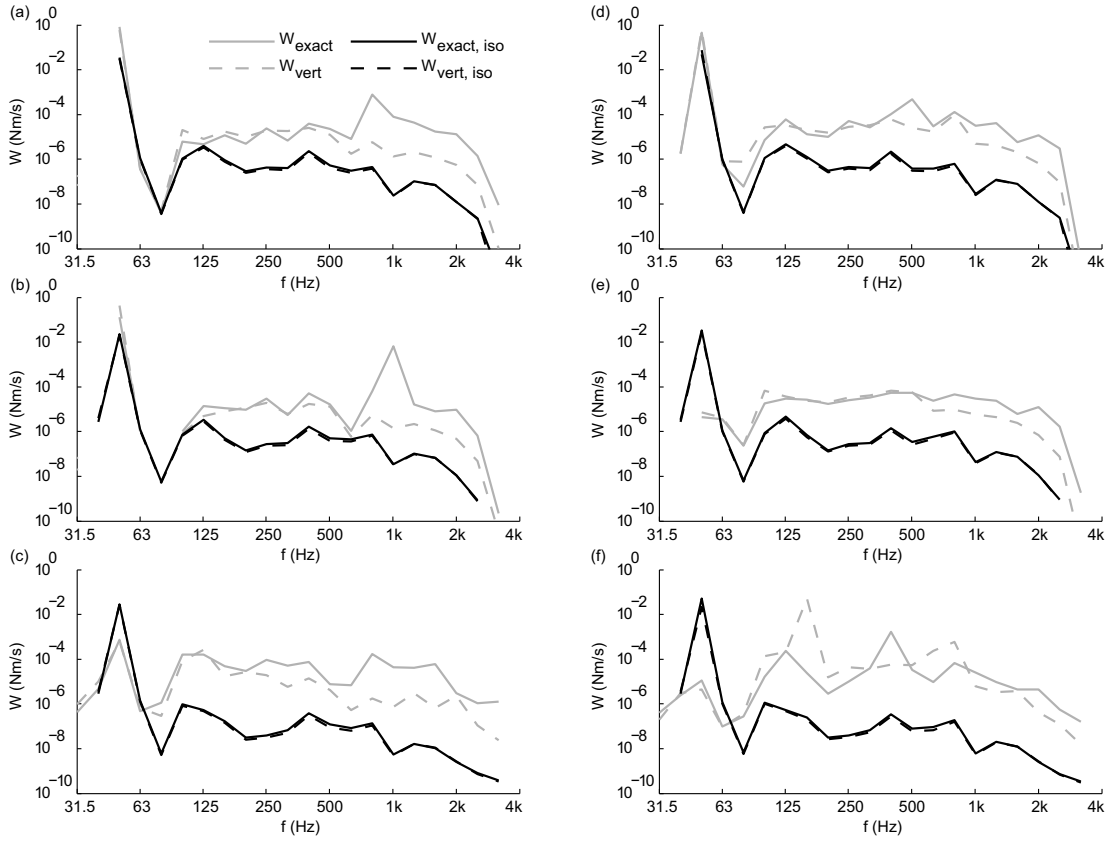

FIGURE 3: Transmitted power from fan source: (a), (b), (c) Interfaces 1,2,3 and (d), (e), (f) Interfaces 1,2,3 with aluminum feet attached

A second (fictitious) contact condition was considered where additional aluminum feet were screwed to the metal sheets of the fan unit frame at the contact point positions, see Fig. 2 (b). The major difference to the first (original) contact condition is that rotatory components of the source mobility now are approximately equal for both rotations, $Y_S^{w_x M_x}$ and $Y_S^{w_y M_y}$. In the original contact condition, both components $Y_S^{w_x M_x}$ and $Y_S^{w_y M_y}$ at a single contact point differ from each other due to the design and curvature of the metal sheets.

Results are shown in Fig. 3 (d) - (f). The overall trend is seen to be similar as in case of the original contact condition. However, the influence of rotatory components in the critical frequency

range from about $f = 800$ Hz onwards is smaller in the rigidly mounted case and amounts to about 10 dB on average. The smallest influence occurs at interface 3, see Fig. 3 (f), where all contact points lie on a joist. Here, rotation around the y-axis is suppressed by the stiffeners (see Fig. 2 (c). At $f = 160$ Hz there is a large overestimate for which no conclusive explanation was found. In the resiliently mounted case, the influence of rotatory components is negligible again.

It can be summarized that a disregard of rotatory components can lead to a large underestimate of the transmitted power in the higher frequency range, irrespective of whether or not the contact points lie on a joist or remote from it in a bay. When the source is resiliently mounted, the influence of rotatory components is negligible.

Single Equivalent Approximation for the Resiliently Mounted Case

In the previous section it was shown that rotatory components can be neglected when the source is resiliently mounted. The transmitted power therefore can be calculated by the translational motion component perpendicular to the structure. In this section, the concept of single equivalent approximation is applied to the resiliently mounted source. The approximate transmitted power was calculated by Eq. (8) for both a zero phase and a random phase assumption, see Eqs. (5) and (6), and compared with an exact calculation obtained by Eq. (3). For any of the interfaces and contact conditions considered, similar results were obtained.

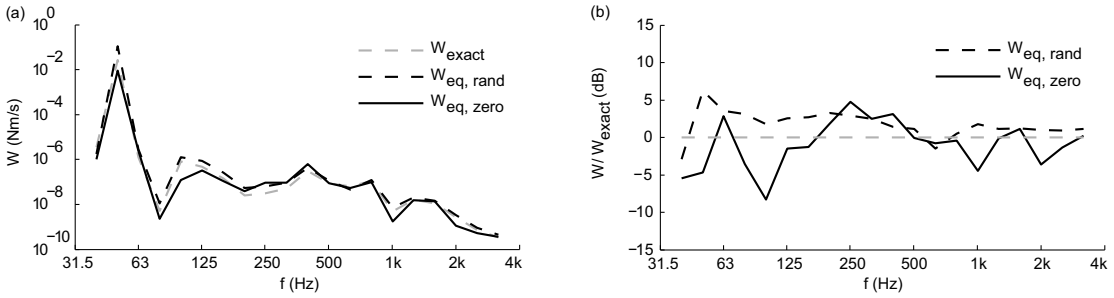

FIGURE 4: (a) Transmitted power from resiliently mounted fan source at interface 3, (b) Normalized power

Exemplarily, results are shown for interface 3 and the original contact condition without aluminum feet attached in Fig. 4. The dashed gray line shows the transmitted power from the exact calculation. The dashed and solid black lines show the approximation with random or zero phase assumption, respectively. For a random phase assumption, the approximation is within a range of ±3 dB throughout the whole spectrum except at $f = 50$ Hz. For a zero phase assumption, errors are within a range of ±5 dB, while a larger error occurs at $f = 100$ Hz. On an overall basis, valuable approximations can be obtained for both phase assumptions.

Significance of Source Mobility

For an effective vibration isolation, isolators must introduce a mobility mismatch between source and receiver. As a rule of thumb, the isolator mobility should exceed the source and receiver mobility by 10 dB. If this condition is fulfilled, the transmitted power becomes invariant of the source mobility terms and they consequently drop out of Eqs. (3) and (8).

In Fig. 5, gray lines, the transmitted power is shown with and without inclusion of the source mobility, calculated by Eq. (3), for interface 3 and the original contact condition without aluminum feet attached. The error is seen to be less than ±2 dB throughout the frequency range. Additionally,

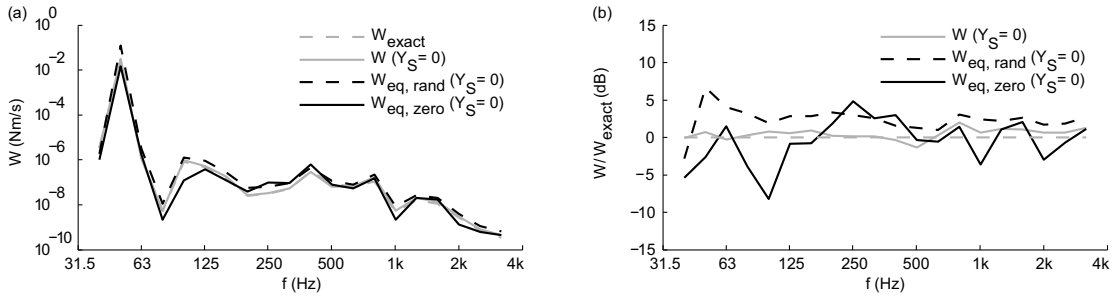

FIGURE 5: (a) Transmitted power from resiliently mounted fan source at interface 3 when source mobility is neglected, (b) Normalized power

results of the single equivalent approximation are shown when source mobilities are neglected (black lines). For both a random as well as a zero phase assumption, results are comparable to those from the previous section where source mobilities are included. Similar results were obtained for the other interfaces and other contact condition considered.

It can be concluded that source mobilities are negligible for both an exact as well as for an approximate calculation of the transmitted power. Consequently, a resiliently mounted source is completely characterized by the free velocity or by the sum of squared free velocities, respectively. Reference is made to international standard ISO 9611 [11] which provides a measurement procedure to determine the approximate free velocity of sources that are resiliently mounted.

CONCLUSION

The multi-component structure-borne sound power transmission from a fan unit source into a continuously welded rib-stiffened aluminum plate was investigated. Based on measurement data, the discrepancy between an exact calculation of power involving the translational component perpendicular to the structure and rotatory components around the in-plane axes of the plate and a calculation reduced to the translational component was derived.

For a rigid coupling of source and receiver, it was shown that rotatory components gain importance with regard to power transmission at about $f = 800$ Hz and above. A neglect of rotatory components, therefore, can lead to an error of 10 dB – 15 dB on average in that frequency range. When the source is resiliently mounted on isolators at each contact point, the influence of rotatory components decreases and an estimation of power from the translational component solely is applicable.

For the resiliently mounted case, the recently proposed concept of single equivalent approximation [3] was applied, leading to single value descriptions of source and receiver data as well as of the isolator subsystem. Furthermore, it was confirmed that the source mobility is of minor importance in the resiliently mounted case and can be neglected. In conclusion, only three parameters are needed to approximate the power transmitted from a resiliently mounted source into a lightweight rib-stiffened plate: First, the source activity has to be accounted for by the sum of the squared free velocity magnitudes. Second, the magnitude of single equivalent receiver mobility and third, the mean isolator mobility have to be estimated.

It needs to be noted that results and conclusions are based on measurement data of three different receiver interface positions as well as two different source feet conditions. Underlying

datasets are rather small compared to the variety of conditions which might be found in practice, thus a generalization must be treated carefully. However, the results may contribute to the knowledge in the field of multi-component structure-borne sound transmission where the database of published case studies is still rather small.

Acknowledgments

The authors would like to thank Dr. Andreas Mayr from the University of Applied Sciences Rosenheim, Germany, for collaborative discussions on the work presented in this paper. The financial support received from the German Federal Ministry of Economics and Technology - BMWi through grant 03SX305G and the technical contribution from Fr. Lürssen Werft Bremen are gratefully acknowledged.

References

[1] B. Petersson, "Structural acoustic power transmission by point moment and force excitation, part 1: beam- and frame-like structures", J. Sound and Vibration **160**, 43–66 (1993).

[2] B. Petersson, "Structural acoustic power transmission by point moment and force excitation, part 2: plate-like structures", J. Sound and Vibration **160**, 67–91 (1993).

[3] A. Mayr and B. Gibbs, "Single equivalent approximation for multiple contact structure-borne sound sources in buildings", Acta Acustica united with Acustica **98**, 402–410 (2012).

[4] B. Petersson and B. Gibbs, "Towards a structure-borne sound source characterization", Applied Acoustics **61**, 325–343 (2000).

[5] P. Gardonio and S. Elliott, "Passive and active isolation of structural vibration transmission between two plates connected by a set of mounts", J. Sound and Vibration **237**, 483–511 (2000).

[6] B. Petersson and J. Plunt, "On effective mobilities in the prediction of structure-borne sound transmission between a source structure and a receiver structure, part 1: Theoretical background and basic experimental studies", J. Sound and Vibration **82**, 517–529 (1982).

[7] B. Petersson and J. Plunt, "On effective mobilities in the prediction of structure-borne sound transmission between a source structure and a receiver structure, part 2: Procedures for the estimation of mobilities", J. Sound and Vibration **82**, 531–540 (1982).

[8] R. Fulford and B. Gibbs, "Structure-borne sound power and source characterization of structure-borne sound sources in multi-point-connected systems, part 1: Case studies for assumed force distributions", J. Sound and Vibration **204**, 659–677 (1997).

[9] A. Elliot, A. Moorhouse, and G.A.Pavić, "Moment excitation and the measurement of moment mobilities", J. Sound and Vibration **331**, 2499–2519 (2012).

[10] R. Bishop and D. Johnson, *The mechanics of vibration* (Cambridge University Press) (1960).

[11] "Acoustics - characterization of sources of structure-borne sound with respect to sound radiation from connected structures - measurement of free velocity at the contact points when resiliently mounted", ISO 9611, International Organization for Standardization, Geneva, Switzerland (1996).